Asia-Pacific Journal of Science and Technology :Volume :30 .Issue :02 .Article ID :.APST-30-02-17. Research Article

APST

Asia-Pacific Journal of Science and Technology

https//:www.tci-thaijo.org/index.php/APST/index

Published by Research Department,
Khon Kaen University, Thailand

Cyanidin-3-O-rhamnoside: A promising inhibitor of the virulence protein subtilisin-like protease-1 in *Microsporum gypseum*

Vijay Lobo[1], Amjath Khan[1], Subhashini Ramakrishnan[2], Ramathilaga Ariyamuthu[2], Balambigai Narayanasamy[2], Bakrudeen Ali Ahmed Abdul[1, *]

[1]Department of Biochemistry, Research Development Cell (RDC), PRIST Deemed University, Thanjavur, Tamil Nadu, India.
[2]Department of Biotechnology, Dr.G.R.Damodaran college of Science, Coimbatore – 641014, Tamil Nadu, India.
* Corresponding author:bakrudeen@prist.ac.in

Received 9 July 2024
Revised 15 August 2024
Accepted 24 September2024

Abstract

Microsporum gypseum, a keratinophilic fungus belonging to the dermatophyte group causes infections of the skin, hair, and nails in humans and animals, leading to conditions such as tinea capitis, tinea corporis, and tinea faciei. Virulence factors play a crucial role in the pathogenicity and subsequent host tissue damage. In dermatopytes, proteases are the primary virulence factors, which facilitate host invasion and utilization of the *stratum corneum*. Unlike most studies targeting the ergosterol biosynthesis pathway for the treatment of fungal infections, this research focuses on a major virulence enzyme, subtilisin-like protease (SUB-1), employing *in silico* evaluation of antifungal compounds against this enzyme. The three-dimensional structure of SUB-1 was retrieved from the AlphaFold database and evaluated using the prediction local distance difference test (pLDDT) scores and a Ramachandran plot. Active site residues were identified based on a literature review and using the webserver ConSurf. Structures of compounds were downloaded from the PubChem database, and the physicochemical properties were analyzed using the Swiss ADME database. Selected compounds were then docked with the SUB-1 by using Glide software, and molecular dynamics simulations were conducted using the Desmond module of Schrödinger for identifying the best-docked complex structure. The results revealed that cyanidin-3-O-rhamnoside exhibits potent activity against SUB-1, with a docking score of -9.4 kcal/mol, binding free energy of -55.23 kcal/mol, and interactions with the active site residues H190, N282, and H342. The efficiency of this compound in inhibiting the growth of *M. gypseum* needs to be validated further using experimental studies.

Keywords: *Microsporum gypseum*, Subtilisin-like protease1, AlphaFold, Cyanidin-3-O-rhamnoside, docking, MD simulation.

1. Introduction

Filamentous fungi, particularly dermatophytes, exclusively infect keratinized tissues like hairs, skin, and nails in humans and animals, leading to dermatophytoses or tinea infections. This group of fungi comprises species of *Microsporum*, *Trichophyton*, and *Epidermophyton* which degrade keratin-rich tissues by producing the proteolytic enzyme keratinase. After hydrolyzing keratin, dermatophytes invade the tissues causing injuries to the host [1]. *Microsporum gypseum* is a geophilic dermatophyte with a widespread distribution worldwide. It utilizes keratinous substrates in soil to colonize, playing a crucial role in keratin degradation [2]. Virulence factors play a crucial role in pathogenicity and play a significant role subsequent tissue damage [3]. The severity of infections varies depending on the host's immune system, the invading virulence factors, infection site, and secondary metabolites produced by the fungus in response to host defences [4]. Dermatophytes secrete virulence enzymes such as lipase, protease, cellulase, and keratinase, each of which exhibit different substrate specificities.

Dermatophytes secrete multiple endoproteases, which belong to two major protein families: subtilisins (serine proteases) and fungalysins (metalloproteases) [5]. In *M. canis*, serine proteases, belonging to subtilisins and

encoded by the genes SUB-1, SUB-2, and SUB-3, serve as virulence factors during the pathogen-induced keratin degradation [6]. These subtilisin-like proteases, enable the fungus to penetrate host tissues and, colonize the skin of the host, as well as provide sustenance to the fungus [7]. In *M. gypseum* subtilis in-like protease 1 (SUB1) catalyzes the breakdown of alpha peptide bonds into polypeptide chains using a catalytic triad mechanism, which includes a serine nucleophile, activated by a proton relay involving acidic residues (aspartate and glutamate) and a basic residue (histidine). The catalytic triad comprises Asp 158, His 190, and Ser 345, which are essential for the function of SUB-1[8].

Natural products from plants, animals, and minerals have been used to treat diseases for centuries [9]. Initially, plants were used directly as medicines; however, since the 19th century, active compounds isolated from medicinal plants have been utilized, leading to the drug discovery process [10]. Medicinal plants are of paramount importance to the traditional medical systems globally. Moreover, knowledge of ethnobotany is crucial for drug research and development. According to the World Health Organization (WHO), 75% of the global population uses herbs and other traditional medicine systems for their healthcare needs [11].

This study investigated various antimicrobial compounds from different medicinal plants for ability to target the virulence protein SUB1 in *M. gypseum*. The anti-dermatophytic activity of these compounds was evaluated through *in silico* molecular docking and molecular dynamics (MD) simulations.

2. Materials and methods

2.1 Protein preparation

Given the nonavailability of the crystal structure of SUB1 of *M. gypseum* (UnipProt Id: E4UPZ4) in the Protein Data Bank, its three-dimensional structure was downloaded from the AlphaFold database [12]. The model quality was verified using the average pLDDT score, exceeded 70, indicating a high degree of confidence. Additionally, the protein structure was assessed using the Procheck server by analyzing residues in a Ramachandran plot [13]. The active sites were identified through a literature review and InterProScan. Moreover, the phylogenetic relationships among homologous sequences were determined using the server ConSurf, which aids in the assessment or nucleic acids within protein, DNA, or RNA molecules [14].

2.2 Compound preparation

Structures of the compounds sourced from natural resources, especially diverse plant parts identified through literature reviews, were retrieved from the PubChem database. The absorption, distribution, metabolism, and toxicity (ADMETox) properties of all phytocompounds were assessed using the Swiss ADME [15].

2.3 Molecular Docking

Protein-ligand docking was executed using the Glide module in Schrödinger, encompassing four key stages: protein preparation, receptor grid generation, ligand preparation, and ligand docking. The protein preparation phase tasks such as addition of hydrogen atoms, determination of bond orders, disulfide bond formations, and refining the alignment of hydroxyl and amide moieties. For energy minimization, the OPLS3e force field was employed, focusing on non-hydrogen atoms, until the average root-mean-square deviation (RMSD) reached the default threshold of 0.3 Å.

A receptor grid was created to surround the active site residues, which were pinpointed through multiple sequence alignments. Ligand optimization was achieved using the LigPrep tool, paired with the OPLS3e force field was utilized in place of ionizer to produce potential ionized and tautomerized structures within a defined pH range. Selected ligands were docked with the pathogen targets through extra precision (XP) docking [16].

2.4 Binding free energy calculation (MM-GBSA)

Based on the structures of the top 10 docked complexes the relative binding free energy was calculated using the Prime module of Schrödinger [17]. The relative binding free energy (ΔG bind) was determined using the following equation:

$$\Delta G_{bind} = E_{complex\ (minimized)} - [E_{ligand\ (unbound,\ minimized)} + E_{receptor\ (unbound,\ minimized)}]$$

2.5 Molecular dynamics simulation

The selected docked complexes from the docking analysis were further analyzed for their structural stability through MD simulations by using the Desmond module in Schrödinger Biosuite. Complexes featuring cyanidin-3-O-rhamnoside with SUB-1 were subjected to MD simulations lasting 50ns. The MD simulations were initiated with system builder tools were used to initiate MD simulations for establishing the solvent model, force field, and boundary conditions.

For the simulations the OPLS 2005 force field was used, and the complexes were placed within a 10 Å boundary and an orthorhombic box. TIP3P water molecules were added to the system [18]. The energy of the complexes was minimized using the steepest descent algorithm as part of the equilibration process in Desmond [19]. Subsequently, the complexes were simulated for 50 ns by using the NPT ensemble class, with the Nose-Hoover chain method for temperature control at 300 K and the Martyna-Tobias-Klein method for pressure coupling at 1 bar [20].

The simulation events were then analyzed, which included calculating the root-mean-square deviation (RMSD) of the protein and ligand bond protein as well as the root-mean-square fluctuation (RMSF) of the protein and ligand. In addition, protein-ligand interactions were examined. These analyses provided insights into the stability of the ligand within the protein's binding site.

3. Results

3.1 Protein preparation

The three-dimensional structure of the protein SUB-1 (E4UPZ4) was downloaded from the AlphaFold database (Figure 1(A)). The structure was validated using the average pLDDT score, which was 83.31, indicating a high-confidence model. Further valuation of the model excellence was performed using a Ramachandran plot, which revealed that 89.5% of the residues were located in the most favored regions (Figure 1(B)). Additionally, the InterPro and UniProt databases annotated the residues D158, H190, L254, G255, N282, S342 and S345 as contributors to the protein's active site. Using the web server conSurf homologous sequences from related species were analyzed to identify conserved residues in SUB-1 (Figure 1(C)).

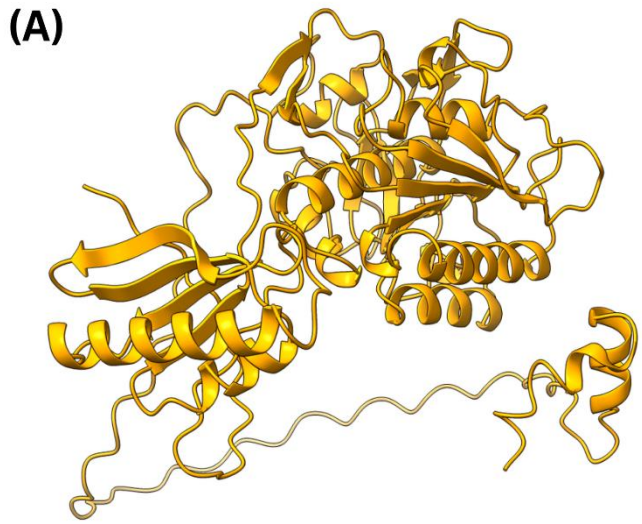

Figure 1 (A) AlphaFold's 3D structure of SUB-1 protein of *M. gypseum* and (B) the structure was validated by analysing the residues of SUB-1 using Ramachandran plot, (C) Identified conserved residues of SUB1 (residues filled with blue color indicates the conservation as variable and dark red color indicates highly conserved,'f' indicates functionally conserved and 's' structurally conserved residues).

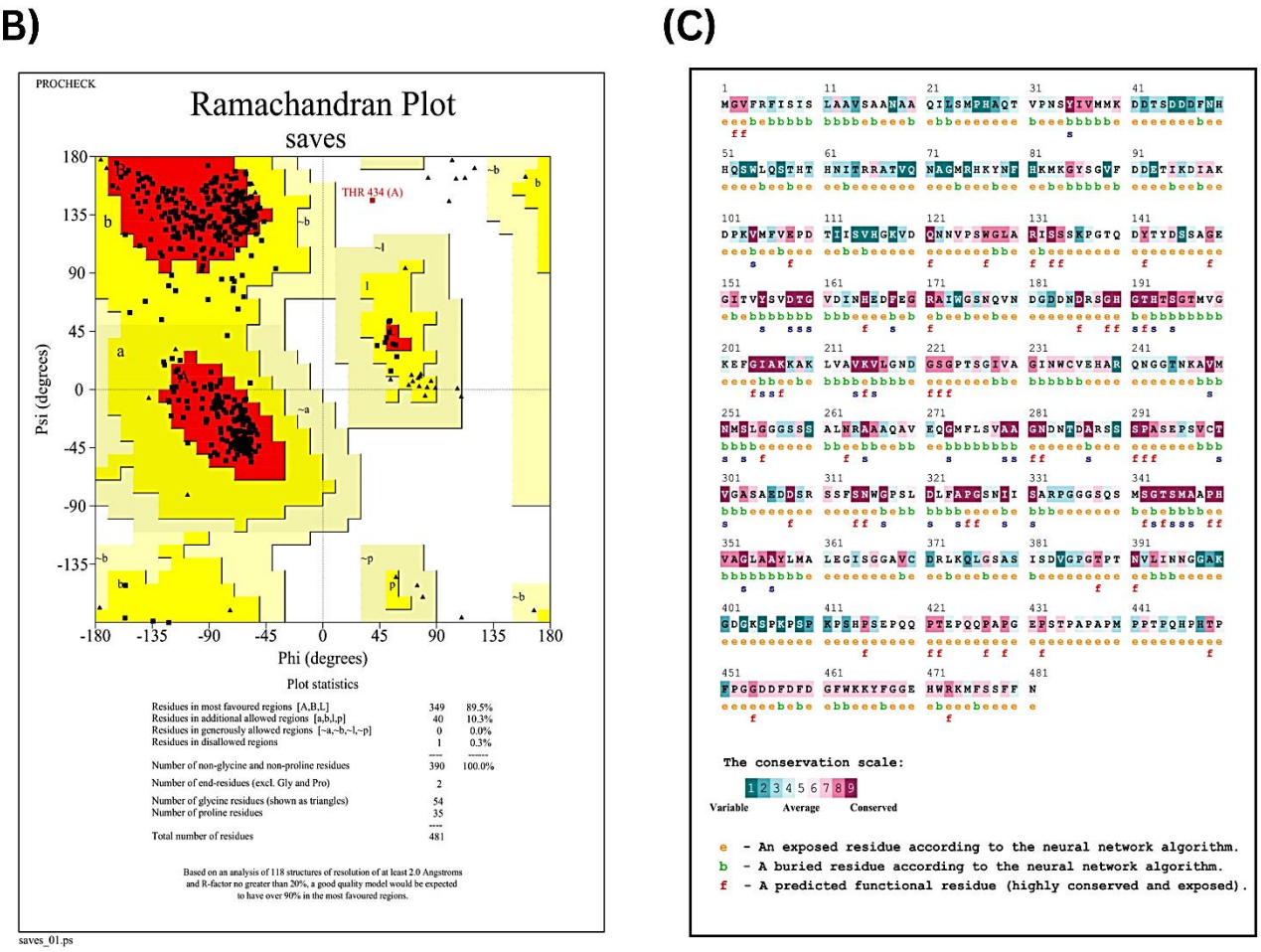

Figure 1 (Cont.)(A) AlphaFold's 3D structure of SUB-1 protein of *M. gypseum* and (B) the structure was validated by analysing the residues of SUB-1 using Ramachandran plot, (C) Identified conserved residues of SUB1 (residues filled with blue color indicates the conservation as variable and dark red color indicates highly conserved,'f' indicates functionally conserved and 's' structurally conserved residues).

3.2 Ligand Preparation

The structures of various phytocompounds with antifungal activities were retrieved from the PubChem database. The selected compounds belonged to diverse classes, including phenols, alkaloids, flavonoids, coumarins, quinones, and saponins. Subsequently, their physicochemical properties and ADMETox characteristics were analyzed. The analysis revealed that kaempferol-3,7-O-α-L-dirhamnoside and tiliroside violated Lipinski's Rule of Five for three times and exhibited poor oral absorption. The remaining compounds complied with the rule and thus were deemed suitable for use as lead molecules (Table 1)

Table 1 Physico-chemical properties of selected anti-fungal compounds from various plants

S.No	Compound Name	MW	HD	HA	MLogP	LogS	HOA (%)	RO5
1.	1,3,6-Trihydroxy-2,5-dimethoxyxanthone	304.25	3	7	2.39	-3.57	High	0
2.	2-(3,4-dimethyl-2,5-dihydro-1H-pyrrol-2-yl)-1-methylethyl pentanoate	239.35	1	3	1.94	-2.08	High	0
3.	3,7-dimethyl-1,6-octadien-3-ol	154.25	1	1	2.97	-2.40	High	0
4.	5,8-dihydroxyumbelliprenin	398.49	2	5	4.73	-4.95	High	0
5.	6,8-didec-(1Z)-enyl-5,7-dimethyl-2,3-dihydro-1H-indolizinium	424.72	0	0	6.54	-8.80	Medium	1

6.	Allolicoiso flavone A	354.35	4	6	4.24	-4.97	High	0
7.	Alpha-cis-ocimene	136.23	0	0	4.33	-3.15	High	0
8.	Angelicin	186.16	0	3	2.08	-2.99	High	0
9.	Antofine	363.45	0	4	4.76	-5.28	High	0
10.	Caledonixanthone E	340.33	2	6	3.70	-4.63	High	0
11.	Cefaclor	367.81	3	5	-1.79	-0.85	High	0
12.	Chlorogenic acid	354.31	6	9	-0.42	-1.62	Medium	1
13.	Cinnamic acid	148.16	1	2	2.13	-2.37	High	0
14.	Conocarpan	266.33	1	2	4.44	-4.60	High	0
15.	Coumaric acid	146.14	0	2	1.39	-2.29	High	0
16.	Cyanidin-3-O-rhamnoside	433.39	7	10	-1.00	-2.38	Medium	1
17.	EGCG	458.37	8	11	1.17	-3.56	Medium	2
18.	Eupomatenoid 3	292.33	0	3	3.34	-5.28	High	0
19.	Eupomatenoid 5	294.34	1	3	2.93	-5.11	High	0
20.	Ferulic acid	194.18	2	4	1.00	-2.11	High	0
21.	Gallic acid	170.12	4	5	-0.16	-1.64	High	0
22.	Hesperetin	302.28	3	6	0.41	-3.62	High	0
23.	Isopinnatal	338.35	1	5	1.09	-3.03	High	0
24.	Kaempferol	286.24	4	6	1.90	-3.31	High	0
25.	Kaempferol-3,7-O-a-L –dirhamnoside	578.52	8	14	-2.69	-3.33	Low	3
26.	Kigelinone	258.23	2	5	2.01	-3.07	High	0
27.	Lapachol	242.27	1	3	1.32	-3.21	High	0
28.	Naringenin	272.25	3	5	0.71	-3.49	High	0
29.	Nitrendipine	360.36	1	6	1.07	-3.60	High	0
30.	Orientin	448.38	8	11	-2.51	-2.70	Medium	2
31.	Quercetin 3-O-alpha-L-rhamnopyranoside	448.38	7	11	0.86	-3.33	Medium	2
32.	Quercetin	302.24	5	7	1.54	-3.16	High	0
33.	quercetin-3,7-dimethyl ether	330.29	3	7	3.04	-4.10	High	0
34.	Resveratrol	228.24	3	2	3.13	-3.62	High	0
35.	Salicylic Acid	138.12	2	3	2.26	-2.50	High	0
36.	Scandenone	404.46	2	5	2.64	-6.24	High	0
37.	Syringic acid	198.17	2	5	0.49	-1.84	High	0
38.	Taurocholic acid	515.70	5	7	2.07	-2.93	Medium	1
39.	Tiliroside	594.52	7	13	-1.04	-4.93	Low	3
40.	Toxyloxanthone C	328.32	3	6	1.01	-4.68	High	0
41.	wighteone	338.35	3	5	1.64	-5.11	High	0

*MW – Molecular weight; HD – Hydrogen bond Donor; HA – Hydrogen bond Acceptor; PlogPo/w – An Octonal-water partition coefficient; PlogS – Water Solubility; HOA – Human Oral Absorption; RO5 – Rule Of Five.

3.3 Molecular Docking

The anti-fungal compounds selected from various plant sources were docked with the protein SUB-1 of *M. gypseum*. The top 10 compounds ranked by their docking score are listed in Table 2. All these compounds interacted with the active site residues Asp158, His190, Leu254, Gly255, Asn282, Ser342, and Ser345 of SUB-1.Notably, cyanidin-3-O-rhamnoside interacted with the active site residues His190, Asn282, Ser342, the functionally conserved residue Gly221, and the residue Asp283, with a docking score of -9.4 kcal/mol (Figure 2A). In addition, epigallocatechin 3-O-gallate (EGCG) (Figure 2B), exhibited a docking score of -8.6 kcal/mol, interacting with the active site residues His190, Gly255, Asn282, Ser345, and other key residues (Table 2). These molecular docking results indicating the interactions of phytocompounds with the virulence factor SUB-1 of *M. gypseum* underscored a strong antifungal activity of the compounds examined.

Table 2 Molecular Docking studies and binding free energy calculation of phytocompounds with SUB-1 protein

S.No	Compound Name	Dock Score (kcal/mol)	Interacting residues	Bond Length (Å)	MMGBSA_dG_Bind (kcal/mol)
1.	Cyanidin-3-O-rhamnoside	-9.4	His190, Gly221, Asn282, Asp283, Ser342	3.98, 2.10, 1.86, 2.32, 1.79	-55.23
2.	EGCG	-8.6	His190, Gly223, Gly255, Asn282, Asp283(2), Ser345	2.14, 1.82, 2.26, 1.91, 1.68, 1.78, 2.07	-50.83
3.	Orientin	-7.9	Gly221, Asp283(2), Ser342	2.02, 2.10, 2.78, 1.85	-48.88
4.	Quercetin 3-O-alpha-L-rhamnopyranoside	-6.8	His190, Ser188, Gly221, Ser342, Ser345	5.04, 2.38, 2.61, 1.89, 1.99	-46.28
5.	Chlorogenic acid	-6.8	His190, Gly221, Ser253, Asn282, Ser342	2.26, 1.81, 1.88, 2.56, 2.03	-35.54
6.	5,8-dihydroxy umbelliprenin	-6.0	Gly223, Gly255, Ser290	2.03, 1.85, 2.54	-41.76
7.	Isopiscerythrone	-6.0	His190, Gly221, Gly255, Ser342	2.30, 2.02, 1.70, 1.83	-44.13
8.	Gallic acid	-5.2	His190, Gly221, Gly255	4.85, 2.08, 2.21	-25.84
9.	Quercetin	-5.2	Ser188, Asn282, Asp283	2.05, 1.87, 2.12	-33.46
10.	Quercetin-3,7-dimethyl ether	-4.8	His190, Asn282, Asp283(2)	4.26, 1.94, 1.92, 1.97	-41.39

3.4 Binding free energy (MM-GBSA) calculation

The binding free energy was computed for every docked structure. Among all structures the complex of cyanidin-3-O-rhamnoside with SUB-1 was identified to have the lowest binding energy at -53.24 kcal/mol, Similarly, EGCG, orientin, and quercetin 3-O-alpha-L-rhamnopyranoside formed complexes with low binding energies (Table 2).

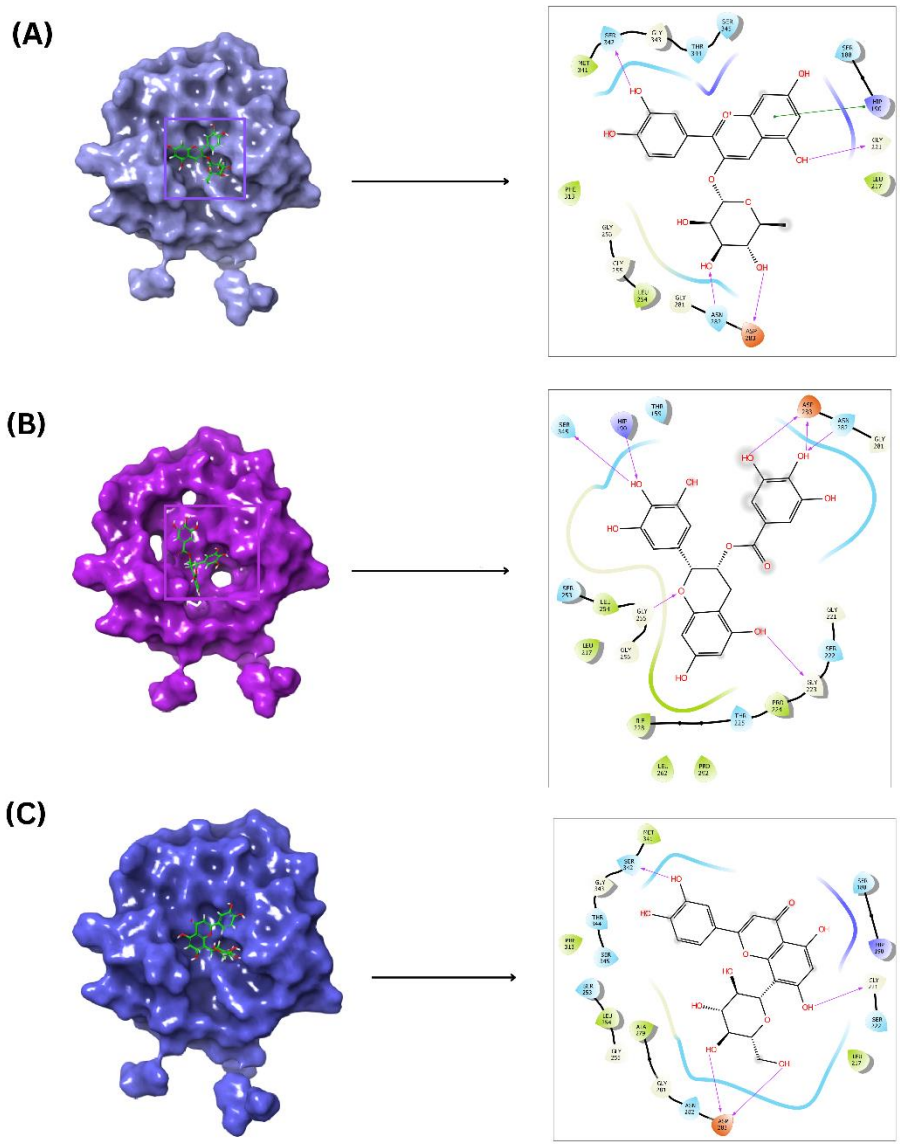

Figure 2 Docked complex structure of Subtilisin-like protease 1 (SUB-1) with (A) Cyanidin-3-O-rhamnoside, (B) EGCG (C) Orientin

3.5 Molecular Dynamics simulation

RMSD values are crucial for predicting stability of the protein and ligand with fluctuations during simulations. The RMSD analysis of the SUB-1 complex indicated that the deviations of both protein Cα atoms and the ligand were within the conventional range of 3.0 Å. Notably, from 16 to 29 ns, the complex exhibited no deviation (Figure 3(A)). RMSF effectively characterizes changes along the protein chain during simulations. In this study, RMSF values for the SUB-1 protein indicated that its C-terminal had greater fluctuations. The residues 217-226 and some loop region residues fluctuated within the range of 3.0 Å (Figure 3(B)).

Protein-ligand interactions during the simulations are represented in the form of a timeline and histogram (Figure 3(C)). The timeline presents the interaction details of each residue throughout the simulation period, whereas the histogram illustrates the types of interactions between the ligand and protein. The analysis revealed that the docked complex of SUB-1 with cyanidin 3-O-rhamnoside formed strong hydrogen bonds with the active site residues Asp158, Ser188, His190, Leu217, Gly218, Asp220, Gly223, Asn282, Asp283, and Ser345. Additionally, the complex formed hydrogen bonds with the residues outside the active site namely Ser188, Gly218, Asp220, Gly223, Asp283, and Ser345 (Figure 3E). The two-dimensional structure analysis showed that active site residues Asp158 (>100%) and Asn282 (86%) had accounted for more than 80% interactions, while Ser188 (30%), Gly255 (41%), Asp283 (62%), and Asp220 (42%) accounted for more than 30% interactions throughout the simulation period (Figure 3(D)).

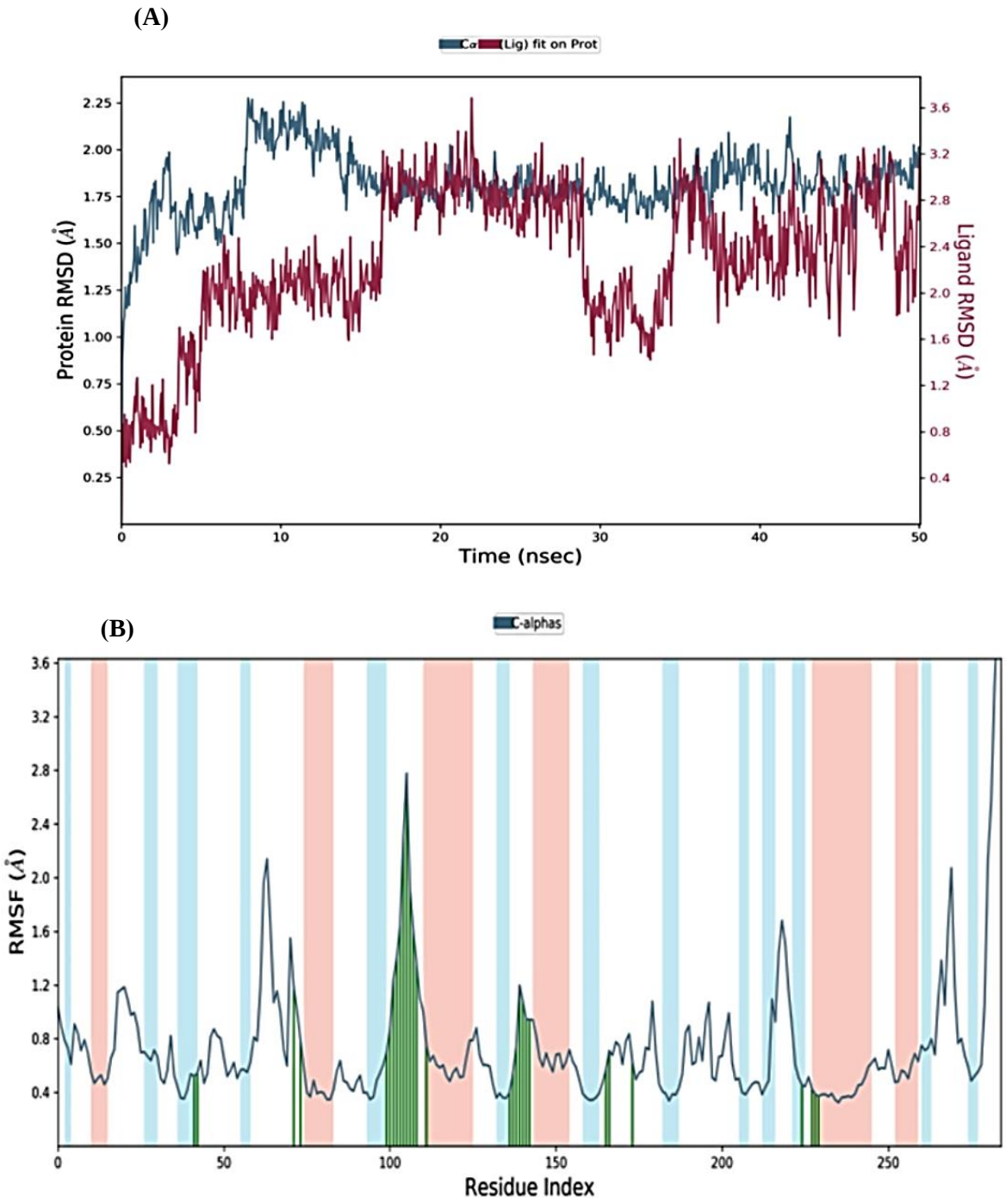

Figure 3 Molecular dynamics simulation studies of complex structure of SUB-1 protein of *M. gypseum* with Cyanidin-3-O-rhamnoside. (A) RMSD plot, blue color indicates protein Cα atoms, and red color heavy atoms of Cyanidin-3-O-rhamnoside (B) RMSF plot of SUB-1 protein, green color lines indicates the interaction of Cyanidin-3-O-rhamnoside (C) Amino acid residues involved in the interaction with compound Cyanidin-3-O-rhamnoside throughout the simulation period, (D) 2D structure of interactions between SUB1 protein with Cyanidin-3-O-rhamnoside at 50th ns, (E)Various types of interactions between protein-ligand complex (green – hydrogen bonds, grey – hydrophobic, blue – water bridges).

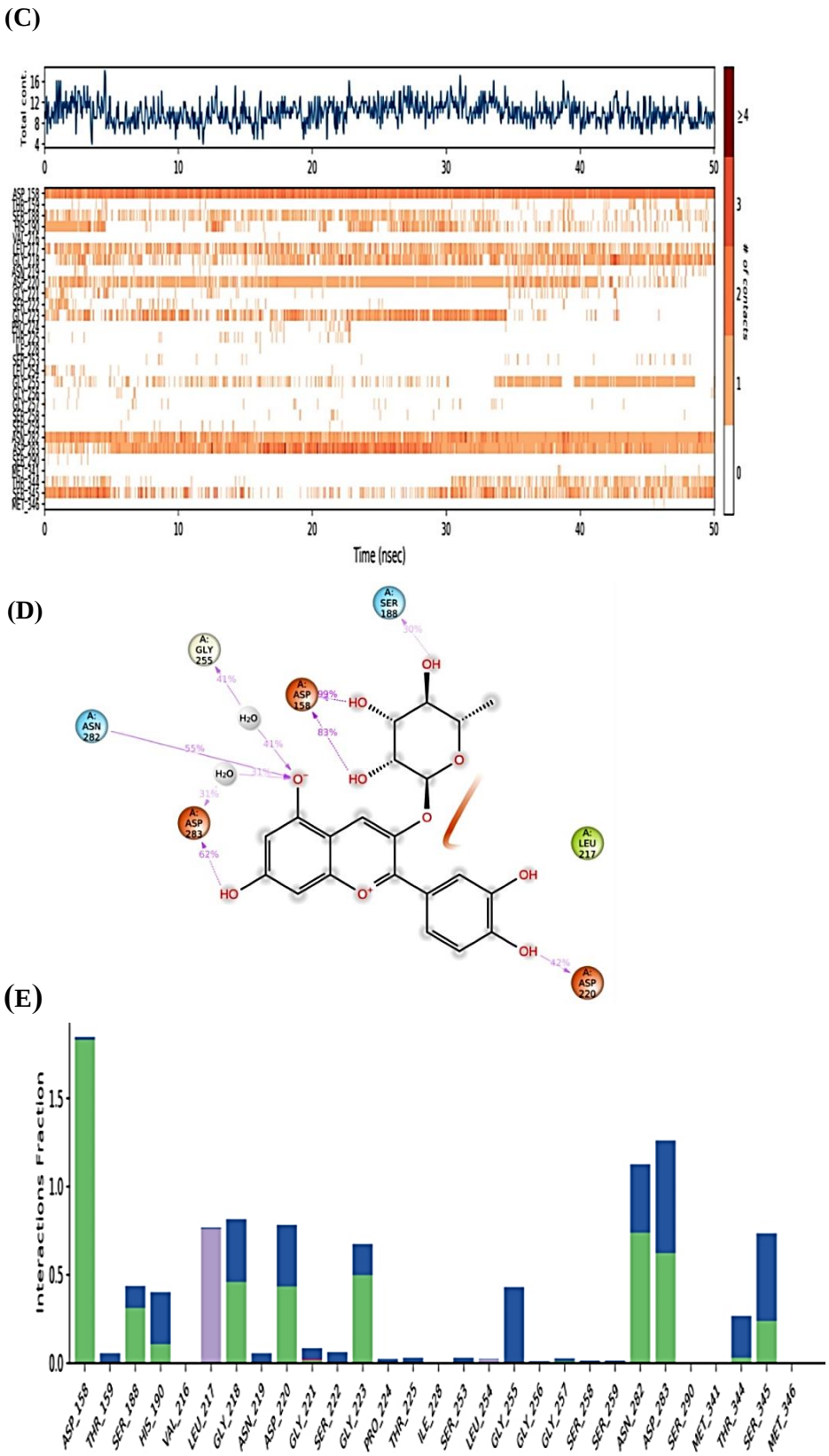

Figure 3 (Cont.) Molecular dynamics simulation studies of complex structure of SUB-1 protein of *M. gypseum* with Cyanidin-3-O-rhamnoside. (A) RMSD plot, blue color indicates protein Cα atoms, and red color heavy atoms of Cyanidin-3-O-rhamnoside (B) RMSF plot of SUB-1 protein, green color lines indicates the interaction of Cyanidin-3-O-rhamnoside (C) Amino acid residues involved in the interaction with compound Cyanidin-3-O-rhamnoside throughout the simulation period, (D) 2D structure of interactions between SUB1 protein with Cyanidin-3-O-rhamnoside at 50th ns, (E)Various types of interactions between protein-ligand complex (green – hydrogen bonds, grey – hydrophobic, blue – water bridges).

4. Discussion

Tinea, also known as dermatophytosis, is a superficial skin infection resulting from dermatophytes, which are a category of filamentous fungi. These organisms are found globally but thrive in warm, humid environments typical of tropical and subtropical areas [21]. Infections by *M. gypseum* typically affect those with soil exposure, like farmers and gardeners, resulting in conditions such as tinea capitis and tinea corporis [22].

Currently, azoles, allylamines, morpholines, and polyenes are a major classes of drug molecules employed for targeting enzymes in the ergosterol biosynthesis pathway to inhibit the growth of dermatophytes [23]; however, many fungi has developed resistance against these drugs. This study concentrated on virulence proteins, particularly subtilisin-like proteases, which are a class of keratinases in dermatophytes responsible for degrading keratin sources, invasion into the host, and pathogenesis [24]. As reported, the virulence of dermatophytes significantly relies on their capacity to secrete these enzymes [25]. Thus, inhibiting SUB-1 may significantly reduce the pathogen's ability to cause disease, making it a valuable target.

The 3D structure of SUB-1 of *M. gypseum* was downloaded from the AlphaFold database, with the average pLDDT score of 83.31 and the Ramachandran plot analysis indicated that 89.5 % of residues were present in the most favoured region, revealing that the structure quality was good. Typically, the pLDDT score ranges between 0 to 100, with a value of pLDDT $\geq$ 90 signifying that the degree of confidence for the prediction of residues is enormously high whereas the values in the range of 90 $\geq$ pLDDT $\geq$ 70 signify a high degree of confidence. Values in the range of 70 >pLDDT $\geq$ 50 indicate a low degree of confidence in the predictions. Predictions with a pLDDT score of $\leq$50 are considered to be of extremely low confidence, suggesting their unreliability or unfeasibility [26]. The prevalence of over 90% of residues in the most favored region indicated that the structural model generated is likely of high quality [27].

Except two all compounds, including cyanidin-3-O-rhamnoside, EGCG, and orientin, adhered to Lipinski's Rule of Five, which qualified them as orally active drug molecules. The Rule of Five is a framework used to assess drug likeness or gauge, whether a compound with specific pharmacological or biological activity has characteristics suitable for oral activity in humans [28]. Molecular docking and simulations demonstrated that cyanidin-3-O-rhamnoside binds to the active site residues Asp158, His190, Gly255, Asn282, Ser342, and Ser345 of SUB-1 in *M. gypseum*. Given the role of the catalytic triad, comprising Asp 158, His 190, and Ser 345, in the enzyme's function, these findings underscore the role of cyaniding-3-O-rhamnoside as a promising inhibitor of M. *gypseum* growth.

Hussain et al. (2019) [29] reported that cyanidin-3-O-rhamnoside, identified in the methanol extract of *B. aegyptiaca* fruits, exhibits antifungal properties and targets proteins in the ergosterol biosynthesis pathway of *M. gypseum* and *T. rubrum*. Additionally, Abuthakir et al. (2021) [30] found that both taurocholic acid and cyanidin-3-O-rhamnoside are effective against the Exocyst complex component protein of *M. gypseum*, a novel drug target. This study reinforces the efficacy of cyanidin-3-O-rhamnoside's against the virulence protein SUB-1. The compound's ability to interact with multiple proteins of the dermatophyte *M. gypseum* underscores; its potential as a multi-targeting agent. Cyanidin-3-O-rhamnoside, EGCG and orientin, all of which belong to the class of flavonoids, demonstrated potent activities against SUB-1. According to Aboody et al. (2020) [31] flavonoids possess the potential antifungal activity against *M. gypseum*, *C. albicans*, among other pathogens, in addition to being safer, cost-effective, and capable of affecting pathogen growth by interfering with the formation of cell wall and plasma membrane, protein synthesis, cell division and other mechanisms. EGCG, another flavonoid compound, exhibits antifungal activity against *C. albicans*, *M. canis*, and *T. Mentagrophytes* [32]. Orientin, extracted from *Piper solmsianum*, demonstrates potential antifungal activity against filamentous fungi like *M. gypseum*, *A. niger*, and *T. rubrum*, and yeast species such as *C. albicans* and *C. tropicalis* [33]. Furthermore, cyanidin-3-O-rhamnoside is found in black currants, common peas, Erythrina vogelii, and the fruit pulp of *Balanitesae gyptiaca* (Abuthakir et al., 2021). EGCG is a major component of green tea [34], whereas orientin is commonly found in fenugreek seeds [35], making these compounds potential biomarkers for the consumption of these foods.

Based on these results, future studies can further evaluate the selected compounds for their efficacy against *M. gypseum* through antifungal and enzyme assays. Additionally, we aim to conduct *in vivo* assays using *Galleria mellonella*, a model organism that shares many similarities with the mammalian immune system for studying infections caused by fungal pathogens.

5. Conclusion

M. gypseum represents a major dermatophytic threat, and curtailing its growth is essential to protect individuals from the stress and inflammation induced by this pathogen. This study focused on SUB-1, a virulence factor critical for *M. gypseum*'s pathogenicity and keratin-rich tissue degradation, though not essential for its survival. The results indicate that targeting SUB-1 protein can be a strategy against dermatophytes, with lower resistance potential and greater specificity toward the causative pathogen. Additionally, this study identified cyanidin-3-O-

rhamnoside, EGCG, and orientin as potential inhibitors of SUB-1. Notably, cyanidin-3-O-rhamnoside exhibited the highest activity against multiple dermatophytic proteins, suggesting its potential as a multi-targeting agent. Further experimental studies are necessary to confirm the anti-dermatophytic efficacy of cyanidin-3-O-rhamnoside.

6.Conflict of Interest

No conflict of interest.

7.References

[1] Simpanya MF. Dermatophytes: Their taxonomy, ecology and pathogenicity. Rev Iberoam Micol. 2000; 17:1-12.

[2] Ginter G.Ecology, epidemiology and clinical symptomatology of infections due *Microsporum gypseum*. Mycoses. 2009; 32(10): 531-535.

[3] Hube BR, Hay J, Brasch J, Veraldi S, Schaller M. Dermatomycoses and inflammation: the adaptive balance between growth, damage, and survival. J Mycol Med.2015; 25(1): e44–58.

[4] AkcaglarS, Ener B, Toker SC, Ediz B, Tunali S, Tore O. A comparative study of dermatophyte infections in Bursa, Turkey.Med Mycol. 2011; 49:602-607.

[5] Monod M. Secreted proteases from dermatophytes. Mycopathologia. 2008; 166(5–6): 285–94.

[6] Descamps F, Brouta F, Monod M, Zaugg C, Baar D, Losson B, Mignon B. Isolation of a Microsporumcanis gene family encoding three subtilisin like proteases expressed in vivo. J Invest Dermatol. 2002; 119: 830-835.

[7] Al-shibly MK, Al-Marshedy AM. Molecular study of virulence factors influencing the pathogenicity of *Trichophyton rubrum*. Ecology, Environment and Conservation. 2019; 25(1): 153-158.

[8] Li J, Li Y, Yang J, Dong L, Tian B, Yu Z, Liang L, Zhang Y, Wang X, Zhang K. New insights into the evolution of subtilisin-like serine protease genes in Pezizomycotina. *BMC Evolutionary Biology*. 2010; 10:1-14.

[9] Suntar I. Importance of ethnopharmacological studies in drug discovery: role of medicinal plants. Phytochem Rev, 2020;19, 1199–1209.

[10] Kinghorn AD. Pharmacognosy in the 21st century. J Pharm Pharmacol. 2001; 53 (2): 135 – 148.

[11] Balakumar S, Rajan S, Thiyagarajan T, Jeeva S. Antifungal activity of *Ocimum sanctum* Linn. (Lamiaceae) on clinically isolated dermatophytic fungi. Asian Pac J Trop Med. 2011; 4(8): 654-7.

[12] Varadi M, Anyango S, Deshpande M, Nair S, Natassia C, Yordanova G, Yuan D, Stroe O, et al. Alpha fold protein structure database: massively expanding the structural coverage ofprotein-sequence space with high-accuracy models. Nucleic Acids Res 2022; 50: D439–D444.

[13] Laskowski RA, MacArthur MW, Moss DS, Thornton JM. PROCHECK – a program to check the stereochemical quality of protein structures. J Appl Crystallogr. 1993; 26 (2):283–291.

[14] Ashkenazy H. et al.ConSurf 2016: An improved methodology to estimate and visualize evolutionary conservation in macromolecules. Nucleic Acids Res. 2016; 44(W1): W344-50.

[15] Riyadi PH, Romadhon, Sari ID, Kurniasih RA, Agustini TW, Swastawati F, Herawati VE Tanod WA. Swiss ADME predictions of pharmacokinetics and druglikeness properties of small molecules present in Spirulina platensis. Conf. Ser.: Earth Environ. Sci., 2021; 890.

[16] Castro-Alvarez A, Costa AM, Vilarrasa J. The performance of several docking programs at reproducing protein–macrolide-like crystal structures. Molecules. 2017; 22 (136), 1–14.

[17] Wang E, Sun H, Wang J, Wang Z, Liu H, Zhang JZH, Hou T. End-Point Binding Free Energy Calculation with MM/PBSA and MM/GBSA: Strategies and applications in drug design. Chem Rev. 2019; 119:9478-9508.

[18] Blessy JJ, Sharmila DJS. Molecular simulation of N-acetylneuraminic acid analogs and molecular dynamics studies of cholera toxin-Neu5Gc complex. J Biomol Struct Dyn. 2014; 33(5): 1126-1139.

[19] Fu Y, Zhao J and Chen Z. Insights into the molecular mechanisms of protein-ligand interactions by molecular docking and molecular dynamics simulation: A case of oligopeptide binding protein. Comput Math Methods Med. 2018; 3502-14.

[20] Peng Y, Yang Y, Li L, Jia Z, Cao W Alexov E. DFMD: Fast and effective Delphi force steered molecular dynamics approach to model ligand approach toward a receptor: Application to spermine synthase enzyme. Front Mol Biosci. 2019; 6: 1-12.

[21] Moskaluk AE, VandeWoude S. Current topics in dermatophyte classification and clinical diagnosis. Pathogens. 2022, 11, 957.

[22] Lee WJ, Park JH, Kim JY, Jang YH, Lee S, Bang YJ, Jun JB. Low but continuous occurrence of *Microsporum gypseum* infection in the study on 198 cases in South Korea from 1979 to 2016. Ann. Dermatol. 2018; 30: 427–431.

[23] Hay, R. Therapy of Skin, Hair and Nail Fungal Infections. J Fungi. 2018. 4(99): 1-13.

[24] Descamps F, Brouta F, Monod M, Zaugg C, Baar D, Losson B, Mignon B. Isolation of a *Microsporumcanis* gene family encoding three subtilisin like proteases expressed *in vivo*. J Investig Dermatol 2002; 119: 830-835.

[25] Moallaei H, Zaini F, Rezaie S, Nourbakhsh F, Larcher G. The enzymatic activity and molecular characterization of a secreted subtilisin-like protease in *Microsporumgy pseum* and *Tricho phytonvan breuseghemii.* Iranian J Publ Health. 2009; 38: 25-33.

[26] Jumper J, Evans R, Pritzel A, Green T, Figurnov M, Ronneberger O, Tunyasuvunakool K, Bates R, Žídek A, Potapenko A, et al. Highly accurate protein structure prediction with Alpha Fold. Nature.2021; 596: 584–589.

[27] Mishra P, Wardhan V, Pandey A, Chakraborty S, Garg G, Chakraborty N. Comparative analysis of sequence-structure function relationship of the SUN-Domain Protein CaSUN1. J Phylogenetics Evol Biol. 2017; 5:3.

[28] Lipinski CA, Lombardo F, Dominy BW, Feeney PJ. Experimental and computational approaches to estimate solubility and permeability in drug discovery and development settings. Adv Drug Deliv Rev. 1997; 23:3-25.

[29] Hussain MSA, Velusamy S, Muthusamy J. Balanitesaegyptiaca (L.) Del. for dermatophytose: Ascertaining the efficacy and mode of action through experimental and computational approaches. Inform Med Unlocked 2019; 15:1-11.

[30] Abuthakir MHS, Sharmila V, Jeyam M. Screening *Balanitesaegyptiaca*for inhibitors against putative drug targets in *Microsporum gypseum*– Subtractive proteome, docking and simulation approach. Infect Genet Evol. 2021; 90(3):104755.

[31] Al Aboody MS and Mickymaray S. Anti-fungal efficacy and mechanisms of flavonoids. Anitbiotics. 2020; 9(2): 45.

[32] Park BJ, Taguchi H, Kamei K, Matsuzawa T, Hyon S, Park J. *In Vitro* Antifungal Activity of Epigallocatechin 3- O -Gallate against clinical isolates of dermatophytes. Yonsei Med J. 52(3):535-8.

[33] De Campos MP, Filho VC, Da SilvaRZ, Yunes RA, Zacchino S, Juarez S, Cruz RCB, Cruz AB. Evaluation of antifungal Activity of *Piper solmsianum* C. DC. var.solmsianum (Piperaceae). Biol Pharm Bull. 2005; 28(8) 1527—1530.

[34] Ghoreishi M, Heidari E. Extraction of epigallocatechin gallate from green tea via modified supercritical CO2: Experimental, modeling and optimization. J Supercrit Fluids. 2012; 72:36–45.

[35] Salehi A, Fallah S, Zitterl-Eglseer K, Kaul HP, Surki AA, Mehdi B. Effect of organic fertilizers on antioxidant activityand bioactive compounds of fenugreek seeds in intercropped systems with buckwheat. Agronomy. 2019; 9(7):367.